# Dynamic Modelling and Optimisation of Large-Scale Cryogenic Separation Processes

M. Rodríguez, J. A. Bandoni, M. S. Diaz

Planta Piloto de Ingenieria Quimica - PLAPIQUI (UNS-CONICET)
Camino La Carrindanga Km 7 – (8000) Bahia Blanca, ARGENTINA
Tel.: +54 291 4861700 Fax: +54 291 4861600
e-mail: {marodriguez,abandoni,sdiaz@plapiqui.edu.ar)

In this work, the open loop dynamic optimisation of a large-scale natural gas processing plant is performed. A rigorous differential-algebraic equation (DAE) model has been formulated to represent main plant units, such as shell and tube heat exchangers, high-pressure separator and demethanizing column. In the shell and tube heat exchangers, the hot stream partially condenses and equations to consider the partial condensation of the fluids have been included. A rigorous index one model for the demethanizing column has been developed. The DAE optimisation problem is solved with a simultaneous approach, in which both state and control variables are discretised and the original DAE optimisation model is transformed into a large-scale nonlinear problem (NLP), which is solved using Sequential Quadratic Programming (SQP) methods. Optimal profiles have been obtained for main operating variables to achieve an enhanced product recovery.

## 1. Introduction

Dynamic modelling and optimisation of chemical processes are currently accepted due to the broad range of benefits that can be derived from their application. However, dynamic optimisation of entire plants has not been addressed until the end of the last decade, mainly due to the lack of reliable large-scale dynamic optimisation algorithms. Cervantes and Biegler (1998) proposed an advanced simultaneous strategy to address these problems; Cervantes et al. (2000) applied this methodology to the dynamic optimisation of a polyethylene plant. More recently, Diaz et al. (2003) analyzed optimal switching between operating modes in cryogenic distillation columns through the formulation of a rigorous dynamic optimisation model including predictions of carbon dioxide precipitation conditions at each stage in the column. Raghunathan et al. (2004) extended the model to account for phase verification through the inclusion of MPECs (Mathematical Programs with Equilibrium Constraints). The transient responses of countercurrent heat exchangers have been studied by Romie (1984), Shah (1981), Lakshmanan and Potter (1994) and more recently by Yin and Jensen (2003). The dynamic optimisation model for heat exchanger with phase change has not been developed in detail due to the complexity of the system.

In this work, we have developed models for dynamic optimisation of cryogenic plants key units, including cryogenic heat exchangers, high-pressure separation tanks and

distillation columns. They comprise differential energy and mass balances, hydraulic correlations and rigorous thermodynamic predictions with SRK (Soave, 1972) equation of state for equilibrium calculations for main units. Special attention has been devoted to countercurrent heat exchangers, which are represented as a multicell model, taking into account partial condensation of natural gas. The differential-algebraic equation (DAE) optimisation problem is transformed into a large-scale nonlinear programming (NLP) problem by collocation on finite elements (Biegler et al., 2002). The resulting problem is solved using a reduced space interior point algorithm. The solution of the DAE optimisation problem provides state and control variables temporal and spatial profiles.

## 2. Process Description

The cryogenic train is the most important part of a turboexpansion natural gas plant. In this sector, inlet gas is cooled in countercurrent cryogenic heat exchangers with residual gas and in demethanizer side and bottom reboilers. The partially condensed gas feed is then sent to a high-pressure separator. The vapor is expanded through a turboexpander to obtain the low temperatures required for high ethane recovery and is then fed to the top of a demethanizer column. The liquid from the high pressure separator enters the demethanizer at its lowest feed point. Methane and nitrogen constitute top product and ethane and heavier hydrocarbons are obtained as bottom product. Carbon dioxide is distributed between top and bottom streams. In this work, the cryogenic sector of the turboexpansion plant has been modeled, where core units are cryogenic heat exchangers, turboexpander and demethanizing column.

## 3. Optimization Algorithm and Model Equations

Model equations have been formulated within a simultaneous dynamic optimisation approach, including the calculation of analytical function derivatives. In countercurrent heat exchangers, fluid temperatures vary not only along the heat exchanger but also with time at each point along the exchanger. This process is modelled by a partial differential equations (PDE) system and algebraic equations. In this work, this PDE system is transformed into an ordinary differential equations (ODE) system by finite differences. Consequently, the resulting dynamic optimisation model includes a DAE system that is transformed into an NLP problem through a full discretisation of state and control variables. The NLP solver is IPOPT (Waechter et al., 2002), which is a barrier method that proceeds by solving a relaxed tolerance, for decreasing values of the barrier parameter. The algorithm applies a Newton method to this system in the reduced space. A detailed description of the models is given below.

Cryogenic heat exchangers are baffled shell-and-tube single-pass counterflow ones, in which the fluid in the tubes is residual gas (mainly methane), and the fluid in the shell is natural gas. There are two consecutive heat exchangers and partial condensation of natural gas takes place within the second one. Figure 1 shows the diagram of the heat exchangers and the high-pressure separator. An effective way to model a shell-and-tube heat exchanger with baffles is to break it up into several linked subsystem or cells. The

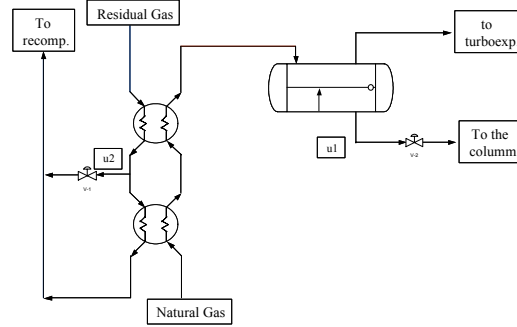number of baffles in the shell and the number of tube passes determine the number of cells.



Figure 1. Cryogenic heat exchangers and high pressure separation tank

*Tube side equations*

The fluid in the tubes is the demethanizer top product (residual gas). Differential energy balances are formulated at cell $i$:

$$\frac{dT_{t,i}}{dt} = \frac{v_{t,i}}{\Delta z} * \left(T_{t,i-1} - T_{t,i}\right) + \frac{U_0 * A_{sup}}{\rho_{t,i} * Cp * A * Long} * \left(T_{s,i} - T_{t,i}\right) \tag{1}$$

Algebraic equations incorporate the functionality of the density, the compressibility factor and the velocity with temperature in each cell.

$$\rho_{t,i} = \frac{Pmol_t * P_t}{Z_{t,i} * Rgas * T_{t,i}} \tag{2}$$

$$v_{t,i} = \frac{G_i * Pmol_t}{\rho_{t,i} * A_t} \tag{3}$$

$$Z_{t,i} = A * T_{t,i} + B \tag{4}$$

with A and B constants.

*Shell side equations*

In the first heat exchanger, where natural gas is cooled, shell side equations are analogous to those describing the tube side. In the second heat exchanger, the proposed model takes into account the partial condensation of natural gas in each cell. It means that each cell is considered as a flash drum with the thermodynamic equations included in each step. Differential equations include energy and mass balances

$$\frac{dH_i}{dt} = Lp_i*hp_i + Vp_i*Hp_i - L_i*h_i - V_i*H_i + Q_{t,i} \tag{5}$$

The algebraic equations include hydraulic correlations; rigorous thermodynamic predictions; geometrical equations and pressure drop correlations. Main algebraic equations are as follows:

Equilibrium ratio for component $k$ ($K_{i,k}$):

$$K_{i,k} = \frac{\phi_{i,k}^{L}}{\phi_{i,k}^{V}} \tag{6}$$

$$y_k = K_{i,k} x_k \tag{7}$$

$$\sum_k K_{i,k} x_k - \sum_k x_k = 0 \tag{8}$$

Vapor ($H_i$) and liquid enthalpies ($h_i$) are calculated as sum of ideal and residual terms:

$$H_i = H^{ideal} - \Delta H \tag{9}$$

These functions, together with fugacity coefficients and compressibility factors for both liquid and vapor phases are calculated with SRK (Soave, 1972) equation of state. The corresponding equations are presented in Rodriguez et al. (2005).

Vapor ($\rho_{V,i}$) and liquid density ($\rho_{L,i}$) are calculated with their compressibility factors

$$P_{s,i} = \frac{\rho_{V,i} * Z_{V,i} * Rgas * T_{s,i}}{Pmol_{V,i}} \tag{10}$$

The exchanger configurations are reported in Table 1. Pressure drop equations considered the correlation from the Bell – Delaware method (1983). In these units optimisation, there are path constraints that correspond to outlet shell side temperature (between 208 and 215 K, high-pressure separator temperature) and outlet tube side temperature (between 303 and 306 K). This condition has been handled through inequalities in the optimisation problem.

Table 1. Heat exchangers configuration

| | | | |
|---|---|---|---|
| Shell internal diam. | $D_s = 0.928$ m | Number of shell pass | $N_{Ts} = 1$ |
| Tube outside diam. | $D_0 = 0.019$ m | Baffle spacing | $L_B = 0.6096$ m |
| Tube pitch | $P_T = 0.0254$ m | Shell length | $L_s = 12.192$ m |
| Array | $\Delta$ (triangular) | Bundle-to-shell diam. clearance | $\Delta_b = 0.0695$ m |
| Number of tubes | $N_T = 990$ | Thickness of baffle | $t_b = 0.005$ m |
| Number of tube pass | $N_{Tp} = 1$ | Baffle cut | 40 % |

The high-pressure separator model includes differential equation for total mass balance. The algebraic equations correspond to vapor volume, liquid and vapor molar holdup, total molar holdup and liquid flow rate.

The demethanizing column model includes dynamic MESH equations, thermodynamic and solubility predictions with SRK equation of state and rigorous hydraulic correlations. Dynamic energy balances are formulated at each stage and vapor holdup is taken into account. The resulting index one DAE system is described in Diaz et al. (2003).

## 4. Numerical Results

The DAE optimisation problem includes 166 differential and 659 algebraic equations and it has been dicretised in 15 finite elements and 2 collocation points. The solution of the resulting NLP has been achieved in 40 iterations. Optimisation variables (liquid flowrate in the high pressure separation tank and natural gas bypass) and main process variables are shown in Figs. 2 to 7 Figures 2 and 3 show the optimal fluid temperature profile in tubes and shell in the heat exchanger, respectively. The profiles increase along the exchanger. They show that temperature reaches steady state in less than 20 minutes. Figure 4 shows the pressure drop profile in each cell of the heat exchanger versus time. The profiles decrease along the heat exchanger due to friction in the baffles.
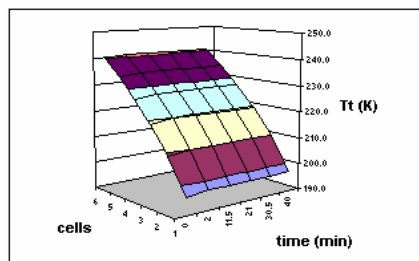
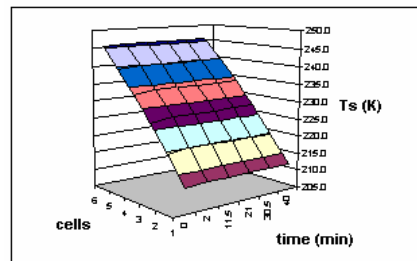Figure 2: Optimal fluid temperature profile in HE (tube side)

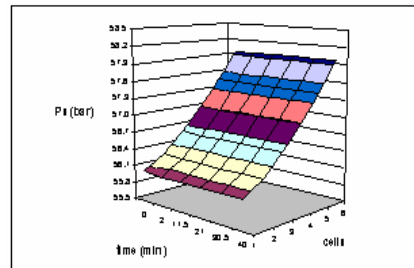Figure 3: Optimal fluid temperature profile in HE (shell side)

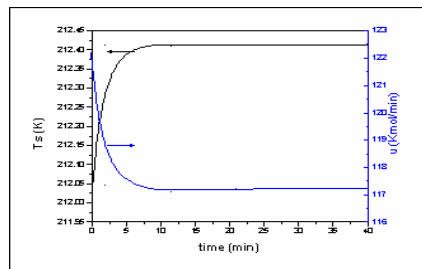Figure 4: Pressure drop profile in HE (shell side)

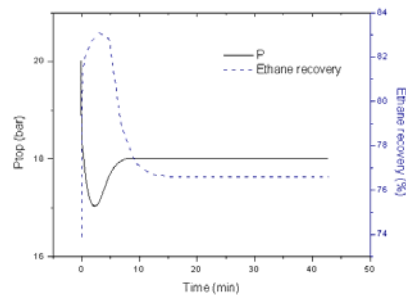Figure 5: Liquid flowrate and fluid inlet temp. profiles in high pressure separator

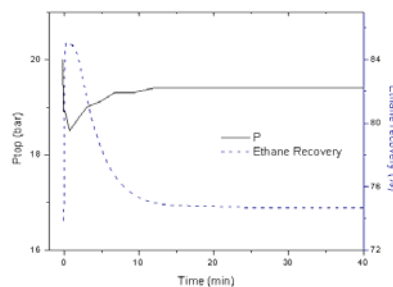Figure 6: Top pressure and ethane recovery profile in distillation column

Figure 7. Optimal profiles for reboiler heat duty in distillation column

Figure 5 shows main optimisation variables in the high pressure separation tank: liquid flowrate decreases to 117.2 kmol/min (from an initial value of 122.1 kmol/min). The

inlet temperature in the tank is 212.4 K in the new steady state. Figures 6 and 7 show different optimisation results for the distillation column when carbon dioxide solubility constraints are ignored and when they are taken into account, respectively. Demethanizing pressure (optimization variable) is decreased to 17.66 bar (from an initial value of 20 bar), rendering 76.6% ethane recovery in the new steady state (Fig. 6). When solubility constraints are included in the model, demethanizing pressure is decreased to 19.2 bar to avoid carbon dioxide precipitation, with a consequent decrease in the new ethane recovery to 74.4% (Fig. 7).

## 6. Conclusions

A rigorous model for the cryogenic heat exchangers, high-pressure separator and demethanizing column from a natural gas processing plant has been presented. The dynamic models for the second heat exchangers, where natural gas partial condensation takes place, have required special effort. The proposed model has considered each cell as a flash drum with the thermodynamic equations included in each step. Carbon dioxide solubility calculation in both liquid and vapor phases at each column stage has been addressed to keep the process within the feasible operating region. The DAE optimisation problem has been solved with a simultaneous approach with advanced mathematical programming techniques. This strategy has allowed the inclusion of path constraints, as residual gas outlet temperature, in the transient. Model resolution provides optimal temporal and spatial profiles, which are in agreement with available data.

### Nomenclature

A: heat transfer area ($m^2$); Asup: Superficial area per length ($m^2$/m); Cp: heat capacity of fluid (kJ/kmol·K); h: liquid enthalpy (MJ/kmol); H: vapor enthalpy (MJ/kmol); L: liquid flow rate (kmol/min); Long: length of straight tube (m); Q: net rate of heat transfer (MJ/min); t: time (min); T: fluid temperature (K); $U_0$: overall heat transfer coefficient (kW/m2K); v: fluid velocity (m/s); V: vapor flow rate (kmol/min). Subscripts: i: cell; p: previous cell; s: shell; t: tube. Greek symbols: $\rho$: fluid density, (kg/m3); $\Delta z$: length of each cell, (m).

## 7. References

Biegler L. T., A. Cervantes and A. Waechter, 2002, Advances in Simultaneous Strategies for Dynamic Process Optimization, Chem. Eng. Sci., 57, 575-593.

Cao E, 1983, Intercambiadores de Calor. 1st ed. Buenos Aires: Edigem.

Cervantes A. M., A. Waechter, R. Tutuncu and L. T. Biegler, 2000, A Reduced Space Interior Point Strategy for Optimization of Differential Algebraic Systems, Comp. & Chem. Eng , 24, 39-51.

Cervantes A. and L. Biegler, 1998, Large-Scale DAE Optimization using Simultaneous Nonlinear Programming Formulations, AIChE Journal 44, 1038-50.

Diaz S., S. Tonelli, A. Bandoni and L. Biegler, 2003, Dynamic optimization for switching between steady states in cryogenic plants, Foundations of Computer Aided Process Operations, 4, 601.

Lakshmanan C, Potter O., 1994, Dynamic Simulation of a Countercurrent Heat Exchanger Modeling-start-up and Frequency Response, International Communications in Heat and Mass Transfer, 21, 421.

Raghunathan A., S. Diaz and L. Biegler, 2004, An MPEC Formulation for Dynamic Optimization of Distillation Operations, Comp. & Chem. Eng., 28, 2037.

Rodríguez M., A. Bandoni and S. Diaz, 2005, Dynamic Optimisation Model for Heat Exchanger with Phase Change, Energy Conversion and Management, Submitted for publication.

Romie F. E., 1984, Transient response of the counterflow heat exchanger, J. Heat Transfer, 106, 620.

Shah R. K., 1981, The transient response of heat exchangers, in: Heat Exchangers: Thermal-Hydraulic Fundamentals and Design. Hemisphere / McGraw-Hill, Washington DC.

Soave, G., 1972, Equil. Constants for a Modified Redlich-Kwong Eq. of State, Chem. Eng. Sci., 27, 1197-1203.

Waechter A, 2002, An interior point algorithm for large-scale nonlinear optimization with applications in process engineering, Ph.D. Thesis, USA, Carnegie Mellon University.

Yin J, Jensen, M., 2003, Analytic model for transient heat exchanger response. International Journal of Heat and Mass Transfer, 46, 3255.